stone), a test can be made to determine whether the sequence was an independent trials process or whether it had a memory of one or more steps (*11*). However, if one cannot distinguish multistory lithologies, the empirically determined transition matrix will have zeros down its main diagonal, as follows:

$$\begin{bmatrix} 0 & p_{12} & p_{13} \\ p_{21} & 0 & p_{23} \\ p_{31} & p_{32} & 0 \end{bmatrix}$$

The zeros in the above matrix could arise from a random process in which all repetitions were lumped together, simply because multistory lithologies could not be distinguished.

Empirically determined transition matrices, because they summarize all the probabilities of going from one lithology to another, establish actual sedimentary cycles. However, before modeling can become fully effective, geologists must obtain data for empirical transition matrices such as that obtained by Vistelius (*1*) and implied by de Raaf *et al.* (*12*). Such matrices will permit us to determine, by statistical test, whether or not the depositional processes that produce stratigraphic sections have a memory.

DONALD D. CARR, ALAN HOROWITZ
S. V. HRABAR, KATHLEEN F. RIDGE
ROSALIA ROONEY
W. THOMAS STRAW
WILLIAM WEBB
PAUL EDWIN POTTER
Department of Geology, Indiana University, Bloomington

References and Notes

1. A. B. Vistelius, *Dokl. Akad. Nauk SSSR* **65**, 191 (1949).
2. C. Allègre, *Bull. Soc. Géol. France* **6**, 214 (1964).
3. F. J. Pettijohn, P. E. Potter, R. Siever, *Sandstone Research Symposium* (Univ. of Alberta, Edmonton, May 1964).
4. A. B. Vistelius and A. V. Faas, *Dokl. Akad. Nauk SSSR* **164**, 40 (1965).
5. ———, *ibid.*, p. 77.
6. A. B. Vistelius and T. S. Feygel 'son, *ibid.*, p. 20.
7. J. C. Griffiths, *Mineral Ind. J.* **35**, 5 (1966).
8. J. W. Harbaugh, *Kansas Geol. Surv. Computer Contrib. No. 1* (1966).
9. G. S. Visher, *Amer. Ass. Petrol. Geol. Bull.* **49**, 1, (1965).
10. J. G. Kemeny and J. L. Snell, *Finite Markov Chains* (Van Nostrand, Princeton, N.J., 1960), p. 70.
11. T. W. Anderson and L. A. Goodman, *Ann. Math. Stat.* **28**, 89 (1957).
12. J. F. M. de Raaf, H. G. Reading, R. G. Walker, *Sedimentology* **4**, 1 (1965).

13. The authors were participants in the Advanced Sedimentation Seminar, Geology, Spring 1966, Indiana University, Bloomington.

14. We thank K. Alam, R. F. Blakely, C. R. Blyth, and J. L. Doob for their assistance.

25 July 1966

Magnetic Anomalies over the Pacific-Antarctic Ridge

Abstract. *Four magnetic profiles across the Pacific-Antarctic Ridge reveal magnetic anomalies that show trends parallel with the ridge axis and symmetry about the ridge axis. The distribution of bodies that could cause these anomalies supports the Vine and Matthews hypothesis for the generation of patterns of magnetic anomalies associated with the midocean ridge system. The geometry of the bodies accords with the known reversals of the geomagnetic field during the last 3.4 million years, indicating a spreading rate of the ocean floor of 4.5 centimeters per year. If one assumes that the spreading rate within 500 kilometers of the ridge axis has been constant, reversals of the geomagnetic field during the last 10.0 million years can be determined. This new, detailed history of field reversals accords with observed anomalies over Reykjanes Ridge in the North Atlantic if a spreading rate of 1 centimeter per year is assumed there.*

Many have recognized the pattern of magnetic anomalies associated with midocean ridges: Heezen *et al.* (*1*) first described the anomaly associated with the Mid-Atlantic Ridge; Ewing *et al.* (*2*) and Heezen *et al.* (*3*) showed the association of this anomaly with the axial region or rift valley; Vine and Matthews (*4*) and Heirtzler and Le Pichon (*5*) have shown generalized linearity of the pattern along the ridge parallel with the axis, and some degree of symmetry across the axis of the ridge. More recently Heirtzler *et al.* (*6*), using data from an aeromagnetic survey of Reykjanes Ridge, have demonstrated more clearly the linearity and symmetry of the anomaly patterns.

To explain the magnetic pattern of the ridges, Vine and Matthews (*4*) hypothesized that material wells up from the ridge axis, becomes magnetized in the direction of the geomagnetic field at the time of cooling below its Curie temperature, and spreads laterally from the axis. Thus the magnetization of the material is parallel or antiparallel to the present direction of the geomagnetic field, depending upon its distance from the ridge axis and the spreading rate. Vine and Wilson (*7*), using the magnetic-reversal history of Cox *et al.* (*8*), have applied the hypothesis to the Juan de Fuca Ridge.

During 1965 U.S.S. *Eltanin* made systematic traverses of the Pacific-Antarctic Ocean between New Zealand and Chile. We now report magnetic measurements from four important traverses of the Pacific-Antarctic Ridge between 40° and 55°S (Fig. 1); the data were acquired with a proton-precession magnetometer system. In Fig. 2 the magnetic-anomaly and bathymetry profiles are projected along an azimuth normal to the axis of the ridge.

The two most striking features of the magnetic profiles are the linearity of the pattern from profile to profile, and the symmetry of the anomaly pattern about the axis of the ridge. To illustrate the linearity, several of the anomalies are assigned numbers (Fig. 2). The axial anomaly 1 to 1′, with its adjacent small anomalies, is prominent in all the profiles and strikingly resembles the axial patterns of the Juan de Fuca Ridge and the Pacific Antarctic [the latter from the *Vema* 16 crossing; see Vine and Wilson (*7*)].

On the eastern ends of the *Eltanin*-21 and northernmost *Eltanin*-20 profiles, anomalies 3′ and 4′ are difficult to identify in a pattern that is quite persistent elsewhere. This distortion may reflect the proximity of the Chile Rise, which can be seen joining the ridge in the northeast corner of Fig. 1.

Lines connect the numbered features

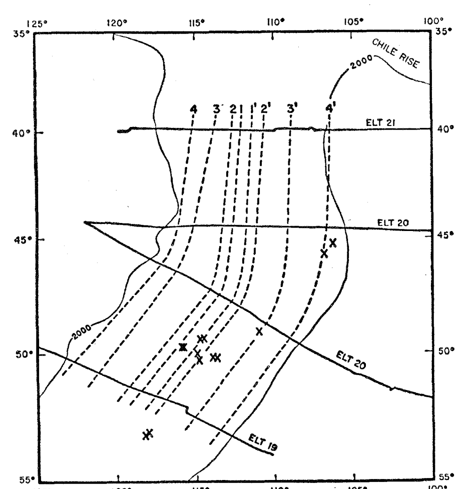

Fig. 1. Ship's tracks in the Pacific-Antarctic Ocean; bathymetric contours in fathoms. The numbers refer to specific magnetic anomalies, and the dashed lines connect similar anomalies. The crosses indicate positions of earthquake epicenters south of 40°S between 1 June 1954 and 31 May 1965 (*18*). *Elt*, *Eltanin.*

in Fig. 1. There is a distinct bend in the anomaly pattern following the bend in the ridge axis at about 47°S: it is in this area, at the western ends of the two *Eltanin*-20 traverses, that the distribution of anomalies is most disturbed. It is felt that a more complete survey at this bend in the ridge would have revealed an in-echelon pattern interrupted by lines of discontinuity, such as exists in the northeast Pacific (*9*).

The symmetry of the central anomaly (1 to 1′) and of the small adjacent anomalies is easily recognized. The general symmetry revealed in the profiles of Fig. 2 is quite apparent by the matches 1 : 1′, 2 : 2′, 3 : 3′, and 4 : 4′.

The most striking instance of symmetry is illustrated in Fig. 3, which shows the *Eltanin*-19 profile both as in Fig. 2, with east on the right-hand side, and reversed, with west on the right-hand side; the bilateral symmetry is revealed in the smallest detail. Anomalies of less than 50 gammas appear in symmetric fashion across the axis of the ridge; the full width of the symmetric region has not been determined. It is clear that the symmetry illustrated in Fig. 3 becomes less exact about 500 km from the axis. A more detailed survey might reveal bilateral symmetry well beyond the axial zone discussed here.

The symmetry of the *Eltanin*-19 profile suggested that the Vine and Matthews hypothesis could be tested by a method similar to that of Vine and Wilson (*7*), who used a uniform spreading rate and the known history of magnetic reversals (*8, 10, 11*). The width of the central anomaly and the spacing of the adjacent four anomalies were correlated with the periods of normal magnetization since the Gilbert reversed epoch; correlation required a spreading rate of 4.5 cm/yr away from the axis. Normally and reversely magnetized bodies were then placed beneath the remaining observed anomalies to the edges of the profile. The depth of the upper surface of the blocks was set by the average bathymetry, and the thickness of the blocks was taken to be 2 km.

Figure 3 also shows the sequence of blocks comprising the full model. The black and white blocks represent normally and reversely magnetized material, respectively. The profile immediately above the model was computed from the model geometry by use of an intensity of magnetization of 5×10^{-3} gauss, an inclination of 60° upward, and a declination of 25°E for the normally magnetized bodies. The magnetization had the same intensity, but the opposite direction, for the reversely magnetized bodies; the strike of the bodies was assumed to be N41°E. To obtain the proper magnitude for the central anomaly, the intensity of magnetization of the central block has been doubled; essentially the same effect could have been obtained by doubling the thickness of the central block, but this would have presented mechanical difficulties as the central block moved toward the less-thick off-axial positions. Why the central block is thus different from the adjacent blocks is not yet clear. Near the edges of the observed profile the anomalies are smaller than those of the model, although both are of the same form; this could mean that the bodies there are slightly less than 2

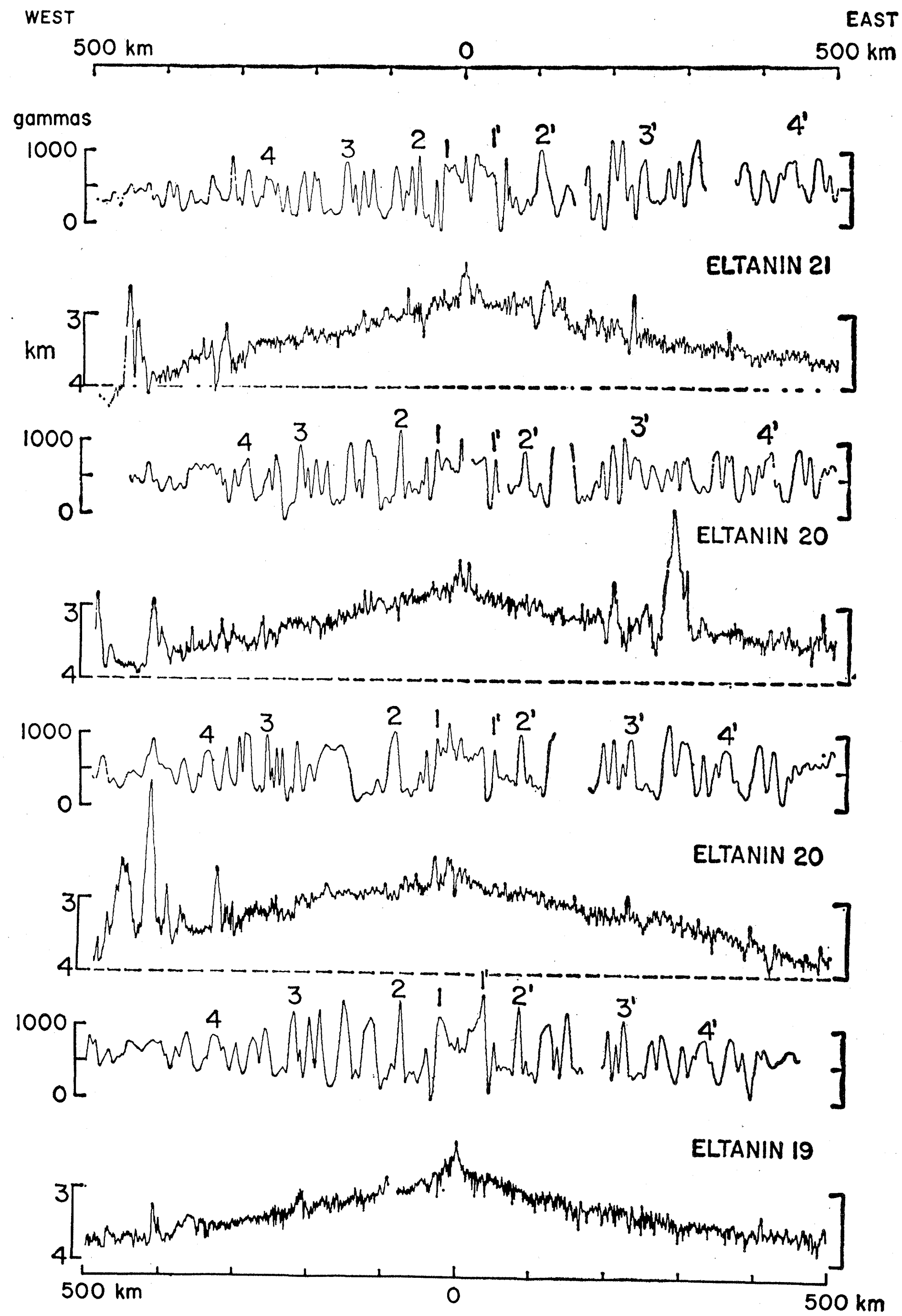

Fig. 2. Observed profiles, of magnetic anomalies and bathymetry, along the tracks shown in Fig. 1; they have been projected along an azimuth at right angles to the ridge axis. The numbers correspond with those in Fig. 1.

km thick, that the magnetization has decreased because of remnant viscous decay, or that chemical alteration has occurred.

The lower part of Fig. 3 includes a time scale related to the distance scale by the spreading rate of 4.5 cm/yr. A history of reversals of the geomagnetic field is thus postulated for the past 10 million years and is given more precisely in Table 1. The two main assumptions on which this history is based are that (i) the process suggested by Vine and Matthews is operative, and (ii) the spreading rate for the last 10 million years was constant for the *Eltanin*-19 traverse. Confirmation of both these assumptions is enhanced if the Pacific-Antarctic model can be applied to another part of the worldwide ridge system, with some adjustment in spreading rate. Heirtzler *et al.* (*6*) observed a high degree of linearity and symmetry of the magnetic pattern associated with Reykjanes Ridge in the North Atlantic. Vine (*12*) has used the history of the geomagnetic field during the past 3.4 million years to determine a rate of spreading for Reykjanes Ridge of about 1 cm/yr; use of this spreading rate contracted the entire Pacific-Antarctic model by a factor of 4.5 in the horizontal dimension but left the thickness of the blocks unchanged. The upper surface of these blocks was made to conform to certain published depths for that area (*13*). The direction and strength of the geomagnetic field appropriate to the area of Reykjanes Ridge were applied.

Figure 4 shows the model, the theoretical anomaly profile that this model produces, and three measured profiles from the aeromagnetic survey of Reykjanes Ridge; the measured profiles were chosen for comparison because they were among the longest and because they were farthest from Iceland and possibly disturbing effects of the Icelandic land mass. Considering the severity of the test for this model, we feel that the similarity of computed and observed profiles is generally good, especially on the eastern side.

There is a good indication that the spreading rates at the *Eltanin*-19 profile and at Reykjanes Ridge have both been constant during the last 10 million years; if not, one would have to assume that the rate changed nearly simultaneously and similarly at both locations. If neither of these hypotheses has been true, it should have been difficult to compare the Pacific Antarctic–body model with observed data from Reykjanes Ridge. It is more reasonable to assume constant spreading rates. There are indications, however, that mechanical constraints such as changes in direction of the ridge axis, juncture with other ridges, or juncture with continental masses can cause the spreading to be obstructed: notice, for example, that anomaly 3 on the western side of the third magnetic profile from the top (Fig. 2) is locally compressed.

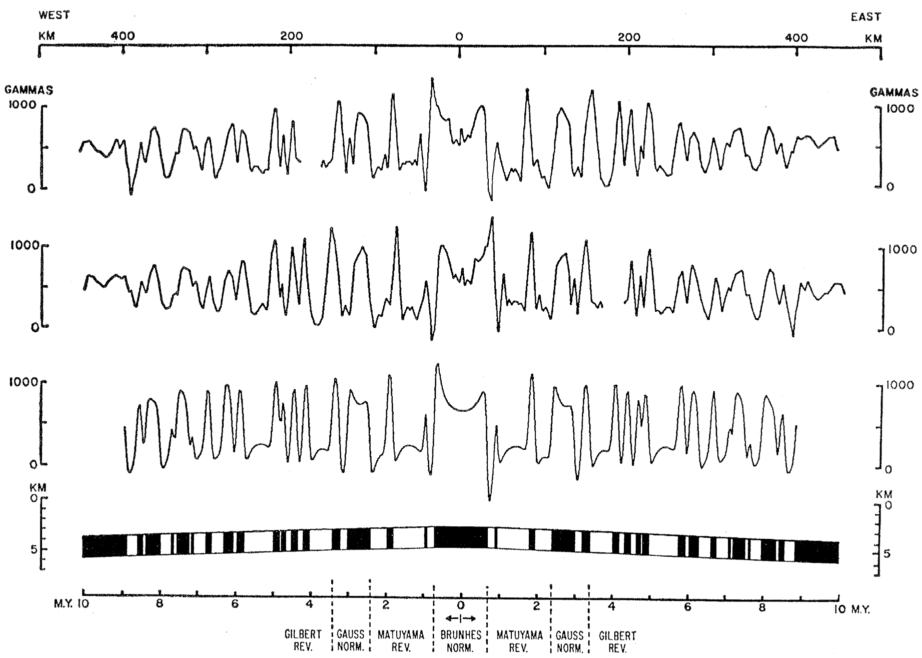

Fig. 3. The middle curve is the *Eltanin*-19 magnetic-anomaly profile; east is to the right. The upper anomaly profile is that of *Eltanin*-19 reversed; west is to the right. On the bottom is the model for the Pacific-Antarctic Ridge. The time scale (millions of years ago) is related to the distance scale by the spreading rate of 4.5 cm/yr. The previously known magnetic epochs since the Gilbert epoch are noted. The shaded areas are normally magnetized material; unshaded areas, reversely magnetized material. Above the model is the computed anomaly profile.

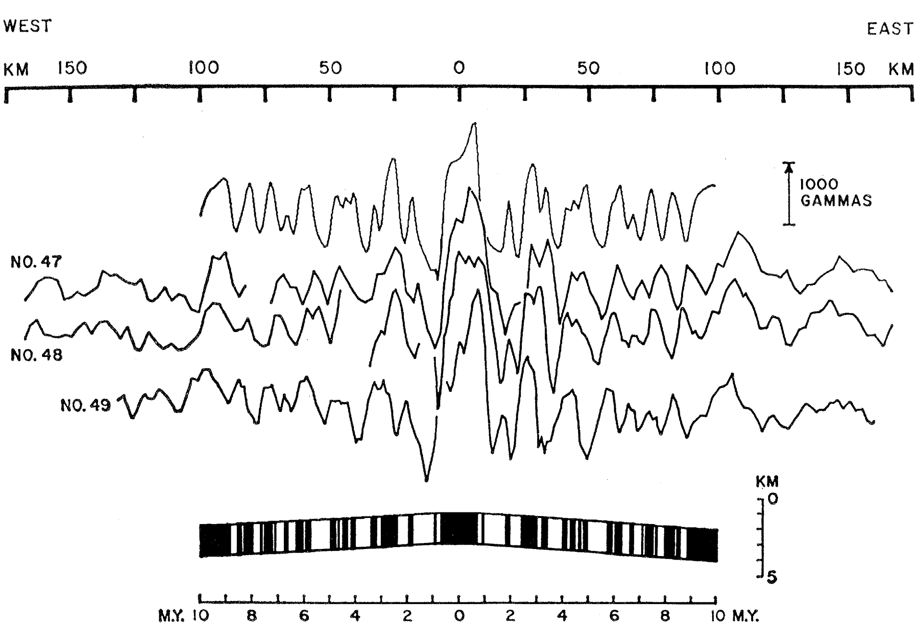

Fig. 4. Bottom shows the Pacific-Antarctic model applied to Reykjanes Ridge, with a time scale related to distance by a spreading rate of 1 cm/yr. The top profile is the one computed from the model. The bottom three profiles are from an aeromagnetic survey of Reykjanes Ridge (*6*); they are projected at right angles to the ridge axis.

Table 1. Periods of normal geomagnetic polarity during the last 10 million years; intervening periods were of reversed polarity.

Millions of years ago		
0.00– 0.70	4.32– 4.47	7.08– 7.12
.90– .95	4.63– 4.74	7.20– 7.51
1.80– 1.95	4.80– 4.95	7.60– 7.66
2.40– 3.00	5.74– 5.92	7.95– 8.33
3.20– 3.40	6.03– 6.27	8.42– 8.55
4.00– 4.16	6.60– 6.74	8.84–10.00

While an isolated ridge segment may or may not change its spreading rate with time, the rate may change with geographic position; the rates of 1, 3, and 4.5 cm/yr quoted for Reykjanes, Juan de Fuca, and Pacific-Antarctic ridges, respectively, illustrate this point. The variation in relative position with respect to the ridge axis of the magnetic anomalies (Fig. 2) indicates the possibility that the spreading rate can change noticeably over the relatively small geographic distance between profiles; this fact allows interpretation of the anomaly patterns in the northeast Pacific. Figure 5 shows types of magnetic patterns that might result from a spreading rate that changed with geographic position along the axis of a ridge but not with time.

Figure 5a shows that a minor variation in spreading rate could create two adjacent anomalies that, although essentially parallel with each other, would not strike parallel with the ridge axis; this condition would exist far from the ridge axis, since near the axis the anomalies would appear parallel not only with each other but also with the axis. If the variation in spreading rate were great enough, anomalies adjacent to the axis would be distinctly nonparallel with the ridge axis (Fig. 5b); this effect could account for the pattern on the eastern side of Gorda Ridge (*14*). Figure 5c shows a discontinuity of spreading rate at a fracture zone; the offset in anomalies across the fracture zone is greatest for the older anomalies and less for the younger. An offset ridge axis, with a discontinuity in spreading rate across a fracture zone, would create similar patterns; such patterns could explain the small variation in offset of the magnetic anomalies across the Mendicino and Pioneer fracture zones.

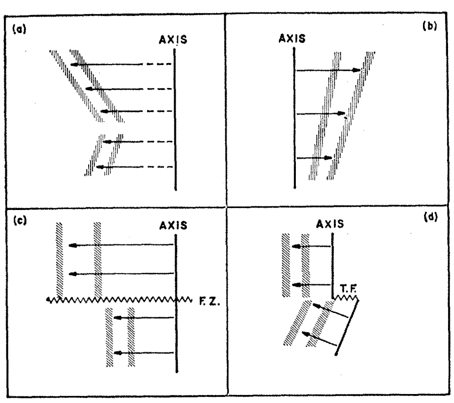

Fig. 5. (a) Shows how a minor variation in spreading rate could create adjacent anomalies (shaded), at a distance from the ridge axis, that are essentially parallel with each other but not parallel with the ridge axis. (b) A large variation in spreading rate close to the ridge axis creates nonparallel anomalies. (c) A difference in spreading rate across a fracture zone (*F.Z.*) creates differences in apparent offset of the anomaly pattern along the fracture zone. (d) Shows how spreading from nonparallel axes of a ridge can produce a disturbed area; the line between the two axial segments is a transform fault (*T.F.*).

Figure 5d shows a constant spreading rate along the axis, but with nonparallel segments of the axis. The juncture of the Juan de Fuca and Gorda ridges (*14*) is reminiscent of this pattern, with epicenters in great density along the transform fault between the offset axes (*14, 15*). Certainly other patterns of magnetic anomalies may be derived by various combinations of axial positions and spreading rates.

Thus the spreading rate of 3 cm/yr found by Vine (*12*) for the Juan de Fuca Ridge is not, we feel, necessarily indicative of the rate for all the northeast Pacific; rather one would expect to find a broken pattern in most areas, like the pattern in the northeast Pacific.

We feel that these results strongly support the essential features of the Vine and Matthews hypothesis and of ocean-floor spreading as postulated by Dietz (*16*) and Hess (*17*). The very rapid apparent-spreading rate in the South Pacific permits one (using a constant spreading rate) to date reversals of the geomagnetic field back to 10 million years ago.

The bodies of the Pacific-Antarctic, when adjusted for slower spreading rate, fit well with magnetic anomalies observed over Reykjanes Ridge in the North Atlantic. Preliminary examination of magnetic data from Gorda Ridge in the northeast Pacific shows (especially on the western side) great similarity to the *Eltanin*-19 profile. Magnetic profiles over the Pacific-Antarctic Ridge in areas other than those discussed by us demonstrate the same similarity. Other magnetic profiles from over the Pacific-Antarctic Ridge, the Indian-Antarctic Ridge (south and southwest of Australia), and the Mid-Atlantic Ridge in the South Atlantic indicate the possible application of this model to those areas.

W. C. PITMAN III
J. R. HEIRTZLER

Lamont Geological Observatory, Columbia University, Palisades, New York

References and Notes

1. B. C. Heezen, M. Ewing, M. T. Miller, *Deep-Sea Res.* **1**(1), 25 (1953).
2. M. Ewing, B. C. Heezen, J. Hirshman, in *Commun. 110-bis Assoc. Seismol. Assemblée Gén. U.G.G.I.* (Toronto, Ontario, 1957).
3. B. C. Heezen, M. Tharp, M. Ewing, *Geol. Soc. Amer. Spec. Paper 65* (1959).
4. F. J. Vine and D. H. Matthews, *Nature* **199**(4897), 947 (1963).
5. J. R. Heirtzler and X. Le Pichon, *J. Geophys. Res.* **70**, 4013 (1965).
6. ———, J. G. Baron, *Deep-Sea Res.* **13**, 427 (1966).
7. F. J. Vine and J. T. Wilson, *Science* **150**, 485 (1965).
8. A. Cox, R. R. Doell, G. B. Dalrymple, *Nature* **198**, 1049 (1963).
9. R. G. Mason, *Geophys. J.* **1**, 320 (1958); A. D. Raff and R. G. Mason, *Bull. Geol. Soc. Amer.* **72**, 1267 (1961); R. G. Mason and A. D. Raff, *ibid.*, p. 1259.
10. R. R. Doell and G. B. Dalrymple, *Science* **152**, 1060 (1966).

N. D. Opdyke, B. Glass, J. D. Hays, J. Foster, *ibid.* **154**, 349 (1966).

12. F. J. Vine, personal communication.
13. Deutsche Hydrographische Inst. chart 256.
14. J. T. Wilson, *Science* **150**, 480 (1965).

M. Talwani, X. Le Pichon, J. R. Heirtzler, *ibid.*, p. 1109.

16. R. S. Dietz, *Nature* **190**(4779), 859 (1961).
17. H. H. Hess, *Petrologic Studies: A Volume in Honor of A. F. Buddington* (Geological Soc. of America, New York, 1962), p. 599.
18. L. Sykes, personal communication.

19. Supported by ONR contract Nonr 266 (48) and NSF grants GA-175 and GP-5536. We thank T. Wustenberg for operating the magnetometer, M. Talwani for use of his computer programs, and F. J. Vine for discussions and reviewing the manuscript. Lamont Geological Observatory contribution 981.

12 September 1966

Copper Artifacts from Prehistoric Archeological Sites in the Dakotas

Abstract. *Thirteen archeological specimens were analyzed spectrographically, and within defined limits they were determined to be native copper. Twelve of the specimens show close elemental homogeneity and are believed to be of Lake Superior ore; the origin of the other specimen is devious.*

Although numerous stone, bone, shell, and vegetal remains from archeological sites on the Northern Plains have been analyzed and identified, only two brief statements have been published which are relative to native copper artifacts from prehistoric sites in